From Shear Centre to Eigenwrenches

Jonathan P. Stacey[a], Matthew P. O'Donnell[b,a], Charles J. Kim[c], Mark Schenk[a,*]

[a] *Bristol Composites Institute (ACCIS), Department of Aerospace Engineering, University of Bristol, Bristol, BS8 1TR, United Kingdom*
[b] *Department of Engineering Design and Mathematics, University of the West of England (UWE Bristol), Bristol, BS16 1QY, United Kingdom*
[c] *Department of Mechanical Engineering, Bucknell University, Lewisburg, PA 17837, USA*

Abstract

In the field of mechanism design, the behaviour of compliant shell mechanisms is commonly characterised via the eigenscrew decomposition of their spatial stiffness matrix. Recent developments have included the design of compliant shell mechanisms made with anisotropic materials. Conceptually, these compliant mechanisms are very similar to morphing composite structures that are typically designed using structural mechanics approaches. Eigenscrew decomposition could, therefore, provide additional insight to designers. To bridge the gap between the two communities, we present the equivalence of eigenscrews (eigenwrench and eigentwist) and familiar structural concepts such as shear centre and centre of twist for the special case of a cantilevered beam. It is hoped that this explicit link will help bridge these disparate fields, and encourage cross-fertilisation of ideas.

Keywords: compliant mechanisms, morphing composites, eigenscrews, screw theory, shear centre

1. Introduction

Compliant mechanisms utilise elastic deformations, instead of links and joints, to achieve a desired response [1]. The behaviour of such mechanisms can be

*Corresponding author
Email address: m.schenk@bristol.ac.uk (Mark Schenk)

non-intuitive, particularly in the case of compliant shell mechanisms, due to the nonlinear dependence on their design parameters. To aid in characterising compliant mechanisms in a more physically intuitive way, the principal compliance axes can be visualised using an eigenscrew decomposition [2, 3]. A library of standard compliant shell mechanisms has since been characterised in such a way, and the relative compliance of their principal translational ('eigenwrench') and rotational ('eigentwist') axes can be compared throughout the mechanism's deformation [4, 5]. By treating these individual mechanisms as building blocks, more complex series and parallel mechanisms can be constructed while still maintaining an intuitive twist-and-wrench design approach [6].

Recent developments using this characterisation technique include compliant shell mechanisms with anisotropic material properties [7]. Using materials with directional stiffness (typical of fibre-reinforced composites) increases the compliant mechanism design space, but also its complexity, making the retention of design intuition valuable. These anisotropic compliant mechanisms designed using screw theory have a lot of overlap with the field of morphing composite structures designed from a structural engineering perspective. Examples of such composite structures include shape-changing plates [8, 9, 10], deployable structures [11, 12, 13, 14, 15, 16], and adaptive aerostructures [17, 18, 19]. As each field converges toward one another, there is great opportunity to mutually leverage insights and methods. The aim of this brief is to offer one such opportunity that has potential to yield mutual benefit to both structural engineers and mechanism designers.

Characterising morphing composites' response via eigenscrew decomposition is typically unfamiliar to structural engineers. However, eigenscrew decomposition could provide structural engineers additional physical insight into the responses thereby encouraging new design approaches. Additionally, Stodieck et al. have highlighted that related structural engineering terminologies can have overlapping definitions and are often confused in literature [20]. Using eigenscrews could provide a clear and consistent characterisation approach.

In this brief we present a derivation that explicitly translates the eigen-

screw concepts from mechanism theory to structural mechanics for the purposes of clarifying and visualising the physical behaviour of a general 3D compliant structure. For a simple structural example, a thin-walled prismatic cantilevered tape spring, we demonstrate analytically that the concepts of shear centre and centre of twist are analogous to the eigenwrench and eigentwist axes, respectively. This insight facilitates the interpretation and application of eigenscrew decomposition in the field of structural mechanics.

2. Shear Centre and Centre of Twist

In structural mechanics, the concept of the shear centre, S, is a well-known property of a prismatic cantilevered beam, derived from the shape of its cross-section. It is defined as the point through which an applied shear loading will not produce a twisting of the beam section; this point need not lie on the beam cross-section itself. Conversely, the centre of twist, T, is defined as the point on the cross-section about which the beam will purely rotate under an applied axial torque (*i.e.* torsion) [21].

For simple beam theory, the position of S and T are found to be equivalent via the Maxwell-Betti reciprocal theory [22, 23, 21]. For a linear-elastic body, the order in which loads are applied does not affect the resulting deformations and strain energy. Consider a shear load F and torsional moment M_z applied to a cantilever beam. The reciprocal theorem shows that the deflection δ at the force application point (and parallel to load F) due to a unit applied moment M_z is equal to the rotation θ_z of the cross-section due to a unit applied load F. If the load is applied at shear centre S, the cross-sectional rotation θ_z is zero; conversely, a torsional moment M_z thus results in no deflection δ at the shear centre, making it the instantaneous centre of twist T. In general S and T need not be coincident: S is determined only from the cross-section geometry, but T also depends on the beam's boundary conditions. For special cases where the beam supports minimise the integral of the torsional warping function over the cross-section these boundary conditions align the two centres [23].

Historically there has been debate in the literature regarding the definitions of shear and twist centres, and reviews of these interpretations and the extent of their differences can be found in Refs [24, 25]. Nevertheless, for the purpose of providing an intuitive interpretation for the "eigenscrews" introduced in the next section, the familiar definitions from simple Euler-Bernoulli beam theory are sufficient.

3. Eigenscrew Decomposition

In mechanism theory, the mechanics of a body is often expressed using "screws". These are derived from Chasles' theorem, which states that any rigid body motion through three-dimensional space can be expressed as a combination of a translation along and rotation about a common axis (the screw axis) [26]. The kinetics of a body can be expressed by screws of combined forces and moments known as "wrenches", and the kinematics can be expressed by screws of combined translations and rotations, known as "twists". Each screw is a 6×1 vector containing information on its position, direction and magnitude.

Lipkin and Patterson introduced a method for characterising the behaviour of a compliant mechanism with a system of "eigenscrews" [2, 3]. By considering a single point of interest (POI), typically an end-effector in the case of a robotic system, a 6×6 tangential stiffness matrix, $\boldsymbol{K}_t$, and compliance matrix, $\boldsymbol{C}_t$, can be formulated. The tangential stiffness matrix can be decomposed into

$$\boldsymbol{K}_t = \begin{bmatrix} \hat{\boldsymbol{w}}_f & \hat{\boldsymbol{w}}_\gamma \end{bmatrix} \begin{bmatrix} \boldsymbol{k}_f & 0 \\ 0 & \boldsymbol{k}_\gamma \end{bmatrix} \begin{bmatrix} \hat{\boldsymbol{w}}_f^T \\ \hat{\boldsymbol{w}}_\gamma^T \end{bmatrix}, \tag{1}$$

and the tangential compliance matrix into

$$\boldsymbol{C}_t = \begin{bmatrix} \hat{\boldsymbol{T}}_f & \hat{\boldsymbol{T}}_\gamma \end{bmatrix} \begin{bmatrix} \boldsymbol{a}_f & 0 \\ 0 & \boldsymbol{a}_\gamma \end{bmatrix} \begin{bmatrix} \hat{\boldsymbol{T}}_f^T \\ \hat{\boldsymbol{T}}_\gamma^T \end{bmatrix}. \tag{2}$$

This decomposition produces three eigenwrenches, $\hat{\boldsymbol{w}}_f$, that describe three principal translational axes, and three eigentwists, $\hat{\boldsymbol{T}}_\gamma$, that describe three principal

rotational axes. The rotational and translational behaviour of the POI are decoupled along these eigenscrew axes. The diagonal matrices $\boldsymbol{k}_f$ and $\boldsymbol{k}_\gamma$ refer to their translational and rotational stiffness respectively; the inverses give compliances $\boldsymbol{a}_f$ and $\boldsymbol{a}_\gamma$.

Assuming some rigid body connects the POI to the axis in question, applying an eigenwrench induces a pure translation of the POI parallel to the eigenwrench axis. Similarly, applying an eigentwist induces a wrench of pure moment about the POI parallel to the eigentwist axis. The $\hat{\boldsymbol{w}}_\gamma$ and $\hat{\boldsymbol{T}}_f$ terms correspond to the induced pure moment wrenches and displacement twists, respectively. Note that eigenscrews (and hence the applied forces or loads) need not necessarily pass through or lie on the structure: a rigid body connects these to the POI. For examples of using this decomposition to characterise compliant mechanisms, see Refs [4, 27, 7].

4. From Shear Centre to Eigenwrench

The shear centre S and centre of twist T characterise how uncoupled translations and rotations can occur in a 2D beam cross-section. Eigenscrews identify the principal translational and rotational compliance axes for a single point on a 3D elastic body. Conceptually, these concepts capture similar behaviours and it follows that S and T may be identifiable from an eigenscrew-decomposition. Centres such as S and T are only valid for simple structural cases (*i.e.* slender, prismatic, isotropic beams). Therefore, if this link can be established for such a case, then eigenscrews could be used by structural engineers to gain insight into more general structures such as those that include material anisotropy, non-prismatic geometries, more complex boundary conditions and geometric nonlinearities.

The selected case study is a cantilevered tape spring, which is a prismatic beam with an open, thin-walled, singly-curved, symmetric cross-section; see Figure 1. The origin is located at the the centroid C and the xy-axes are aligned with the principal axes of the cross-section, such that the bending stiffness is

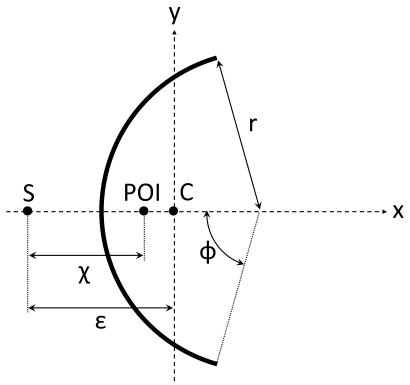

Figure 1: Cross-section of the tape spring. The origin is located at the centroid C and the xy-axes are aligned with the principal axes of the cross-section ($I_{xy} = 0$). The location of shear centre S is defined by distance ϵ from the centroid, and the POI at the cantilever tip lies at distance χ from the shear centre along the symmetry axis.

given by second moments of area I_{xx} and I_{yy} ($I_{xy} = 0$). The z-axis is defined according to the right hand rule. The centroid C is the point on the cross-section through which axial loading produces pure axial extension of the beam. The tape spring cross-section is symmetric about the x-axis, and the position of the shear centre S is given by distance

$$\epsilon = \frac{2r(\sin\phi - \phi\cos\phi)}{\phi - \sin\phi\cos\phi} \tag{3}$$

from the centroid along the symmetry axis [28]. Here, ϕ is equal to half of the cross-section enclosed angle and r is the arc radius. The isotropic tape spring has length L, and is fully fixed (encastre) at the root.

4.1. Compliance Matrix Construction

The POI for the eigenscrew analysis is located at the tip of the cantilever ($z = 0$), and chosen to lie at a distance χ from the shear centre, S, along the x-axis; see Figure 1. The compliance matrix is constructed from first principles of mechanics of materials (assuming Euler-Bernoulli beam theory, and no warping of the cross-section) by considering the response of the POI when forces and moments are applied [29]. Terms are defined with the usual notation: second moments

of area I_{xx} and I_{yy}, beam length L, Young's Modulus E, cross-sectional area A, shear modulus G and polar moment of inertia, J. Moments are defined according to the axis they act around, *i.e.* M_x refers to a moment about the x-axis. This process has been simplified, at no loss of generality, by choosing the cross-sectional coordinate system so that $I_{xy} = 0$. The compliance matrix is then,

$$\left[\begin{array}{c} \delta_x \\ \delta_y \\ \delta_z \\ \hline \theta_x \\ \theta_y \\ \theta_z \end{array}\right] = \left[\begin{array}{ccc|ccc} C_{11} & 0 & C_{13} & 0 & C_{15} & 0 \\ 0 & C_{22} & 0 & C_{24} & 0 & C_{26} \\ C_{31} & 0 & C_{33} & 0 & C_{35} & 0 \\ \hline 0 & C_{42} & 0 & C_{44} & 0 & 0 \\ C_{51} & 0 & C_{53} & 0 & C_{55} & 0 \\ 0 & C_{62} & 0 & 0 & 0 & C_{66} \end{array}\right] \left[\begin{array}{c} F_x \\ F_y \\ F_z \\ \hline M_x \\ M_y \\ M_z \end{array}\right], \tag{4}$$

where the compliance components

$$C_{11} = \frac{L^3}{3EI_{yy}}, \quad C_{22} = \frac{L^3}{3EI_{xx}}, \quad C_{33} = \frac{EA}{L},$$

govern deflections δ due to applied forces F, and

$$C_{44} = \frac{L}{EI_{xx}}, \quad C_{55} = \frac{L}{EI_{yy}}, \quad C_{66} = \frac{L}{GJ},$$

describe rotations θ due to applied moments M. Deflections due to any POI offset from the centroid, C, are given by

$$C_{13} = C_{31} = \frac{(\epsilon - \chi)L^2}{2EI_{yy}}.$$

The coupling between applied forces and resulting rotations (and conversely, applied moments and resulting deflections) is given by

$$C_{15} = C_{51} = \frac{L^2}{2EI_{yy}}, \quad C_{24} = C_{42} = -\frac{L^2}{2EI_{xx}},$$
$$C_{26} = C_{62} = \frac{\chi L}{GJ}, \quad C_{35} = C_{53} = \frac{(\epsilon - \chi)L}{EI_{yy}},$$

where C_{62} reflects rotation around the shear centre (*i.e.* centre of twist) for a transverse load not passing through S.

The compliance matrix is inverted to give the stiffness matrix,

$$\begin{bmatrix} \boldsymbol{K}_1 & \boldsymbol{K}_2 \\ \boldsymbol{K}_3 & \boldsymbol{K}_4 \end{bmatrix} = \begin{bmatrix} \boldsymbol{C}_1 & \boldsymbol{C}_2 \\ \boldsymbol{C}_3 & \boldsymbol{C}_4 \end{bmatrix}^{-1} \tag{5}$$

where the four 3×3 quadrants of the stiffness matrix ($\boldsymbol{K}_1-\boldsymbol{K}_4$) can be found by a piece-wise inversion of the quadrants of the compliance matrix ($\boldsymbol{C}_1-\boldsymbol{C}_4$) using the Schur complement for block matrices (also used to invert $\boldsymbol{ABD}$ matrices in composite plate theory [30]). This results in

$$\boldsymbol{K}_1 = \boldsymbol{P}_1 - \boldsymbol{P}_2\boldsymbol{P}_4^{-1}\boldsymbol{P}_3, \qquad \boldsymbol{K}_2 = \boldsymbol{P}_2\boldsymbol{P}_4^{-1},$$
$$\boldsymbol{K}_3 = -\boldsymbol{P}_4\boldsymbol{P}_3^{-1}, \qquad \boldsymbol{K}_4 = \boldsymbol{P}_4^{-1},$$

with partial inversions

$$\boldsymbol{P}_1 = \boldsymbol{C}_1^{-1}, \qquad \boldsymbol{P}_2 = -\boldsymbol{C}_1^{-1}\boldsymbol{C}_2,$$
$$\boldsymbol{P}_3 = \boldsymbol{C}_2\boldsymbol{C}_1^{-1}, \qquad \boldsymbol{P}_4 = \boldsymbol{C}_4 - \boldsymbol{C}_2\boldsymbol{C}_1^{-1}\boldsymbol{C}_2.$$

Once both the stiffness and compliance matrices are found, the eigenscrew decomposition can be used to find the positions, orientations and magnitudes of the eigenwrench and eigentwist axes.

4.2. Eigenscrew Decomposition Results

The eigenscrew decomposition produces position vectors (relative to the POI) and orientation vectors for the eigentwist and eigenwrench axes. Recall that a load applied along an eigenwrench axis will describe a parallel translation of the POI; similarly, a rotation around eigentwist axes induces a parallel moment at the POI. Inspecting these positions and orientations shows that there are direct links between eigenscrews and the shear centre and centre of twist. Figure 2 shows an isotropic, thin-walled tape spring (POI at the free end centroid) with

eigenscrews and loci of cross-sectional shear centres plotted to help illustrate the analytical link.

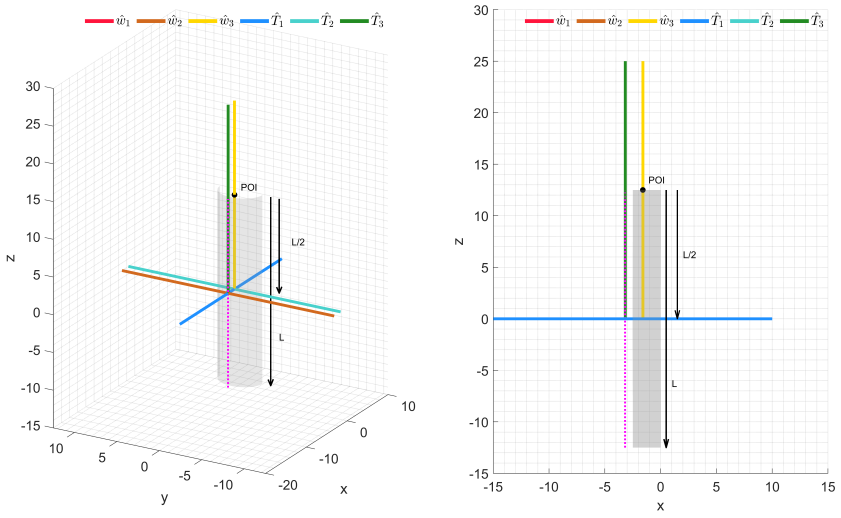

Figure 2: Visualisation of eigenscrews (eigenwrenches $\hat{w}_1$–$\hat{w}_3$ and eigentwists $\hat{T}_1$–$\hat{T}_3$) and shear centre loci (dashed magenta line) for the undeformed tape spring. The tape spring is 5 times as long in the z-direction as it is wide in the y-direction, and has an enclosed angle of 180°

Equations 6–8 show the position vectors $\boldsymbol{r}_w$, orientations $\boldsymbol{f}$ and stiffness magnitudes $\boldsymbol{k}_f$ respectively for the eigenwrenches $\hat{w}_1 - \hat{w}_3$, with each column corresponding to a single eigenwrench:

$$\boldsymbol{r}_w = \begin{bmatrix} 0 & (\epsilon - \chi) & -\chi \\ 0 & 0 & 0 \\ -\frac{L}{2} & 0 & -\frac{L}{2} \end{bmatrix}, \tag{6}$$

$$\boldsymbol{f} = \begin{bmatrix} 1 & 0 & 0 \\ 0 & 0 & 1 \\ 0 & 1 & 0 \end{bmatrix}, \tag{7}$$

$$\boldsymbol{k}_f = \begin{bmatrix} \frac{12EI_{yy}}{L^3} & 0 & 0 \\ 0 & \frac{EI_{yy}L}{AI_{yy}E^2 - L^2\chi^2 + 2L^2\chi\epsilon - L^2\epsilon^2} & 0 \\ 0 & 0 & \frac{12EGI_{xx}J}{GJL^3 - 12EI_{xx}L\chi^2} \end{bmatrix}. \tag{8}$$

Eigenwrench $\hat{w}_1$ exists at a distance $-L/2$ from the POI in the z-direction, orientated parallel to the x-axis. This means — assuming a rigid body connects it to the POI — that a force in the x-direction applied halfway down (and in the centre of) the tape spring will cause a pure translation of the POI in the x-direction; this can be verified readily from beam theory. Eigenwrench $\hat{w}_2$ is located at $\epsilon - \chi$ from the POI in the x-direction (*i.e.* at the centroid C), orientated parallel to the z-axis. This means that a force applied along this eigenwrench axis will cause a pure translation of the POI in the z-axis; thereby demonstrating the definition of the centroid. Finally, eigenwrench $\hat{w}_3$ exists at $-L/2$ from the POI in the z-direction, $-\chi$ from the POI along the x-axis (*i.e.* at S), and is orientated parallel to the y-axis. Similarly to eigenwrench $\hat{w}_1$, it can be seen here that a force applied along $\hat{w}_3$ (*i.e.* through the shear centre, halfway down the tape spring) will cause pure parallel translation of the POI. This result directly links the 2D shear centre concept to a 3D eigenwrench.

Equations 9, 10 and 11 show the position vectors $\boldsymbol{r}_T$, orientations $\boldsymbol{\gamma}$ and compliance magnitudes $\boldsymbol{a}_\gamma$ respectively for the eigentwists $\hat{T}_1$–$\hat{T}_3$, with each column corresponding to a single eigentwist:

$$\boldsymbol{r}_T = \begin{bmatrix} 0 & (\epsilon - \chi) & -\chi \\ 0 & 0 & 0 \\ -\frac{L}{2} & -\frac{L}{2} & 0 \end{bmatrix}, \tag{9}$$

$$\boldsymbol{\gamma} = \begin{bmatrix} 1 & 0 & 0 \\ 0 & 1 & 0 \\ 0 & 0 & 1 \end{bmatrix}, \tag{10}$$

$$\boldsymbol{a}_\gamma = \begin{bmatrix} \frac{L}{EI_{xx}} & 0 & 0 \\ 0 & \frac{L}{EI_{yy}} & 0 \\ 0 & 0 & \frac{L}{GJ} \end{bmatrix}. \tag{11}$$

Eigentwist $\hat{T}_1$ exists at a distance $-L/2$ from the POI in z-direction, orientated parallel to the x-axis. This eigentwist is co-linear with eigenwrench $\hat{w}_1$, and means that a rotation applied around this axis will cause a pure moment about the x-axis at the POI. For an isotropic tape spring with a large enclosed angle, this will have the lowest value of compliance as typically $EI_{xx} > EI_{yy} > GJ$. Eigentwist $\hat{T}_2$ is located at $-L/2$ from the POI in the z-direction, $\epsilon - \chi$ from the POI in the x-axis (*i.e.* at the centroid C), orientated parallel to the y-axis. A rotation about this axis will cause a pure 'tape spring bending' moment about the y-axis at the POI. Finally, eigentwist $\hat{T}_3$ exists at $-\chi$ from the POI along the x-direction (*i.e.* at the shear centre, S), and is orientated parallel to the z-axis. A rotation around this axis will induce a parallel moment M_z about the z-axis at the POI; this corresponds to the definition of the centre of twist T. This matches the result from the reciprocal theorem to show that $T = S$. Aligning the POI with the beam centroid would cause some of the position vector terms to become zero as $\chi = \epsilon$, and for a doubly-symmetric cross-section (as in the beam analysed by Ciblak [31]) the shear centre coincides with the centroid, so that $\chi = 0$.

For the simple case of a cantilevered beam, we have thus shown that the well-known structural concepts of shear centre, S, and centre of twist, T, map to an eigenwrench and eigentwist. This allows structural engineers to interpret the eigenscrew concepts as 'generalised shear centres' and 'axes of twist' which help to interpret the structural response for more general compliant shells. Lastly, it should be noted that S and T are structural concepts derived from beam cross-sections, and while the eigenscrews are applicable to more general 3D structures, they do depend on the location of the applied load.

5. Material Anisotropy and Non-Prismatic Geometry

For a simple case of a cantilevered beam there exists a direct link between these structural and eigenscrew concepts, but as the assumptions of material isotropy and prismatic geometry are relaxed, the shear and twist centres cease being applicable. Instead, eigenscrew characterisation can be valuable by providing a robust framework for gaining insight into the principal translation and rotation axes and their relative compliance for general 3D structures.

To illustrate the advantages of eigenscrew characterisation we consider two case studies: (i) a single-ply composite tape spring where the material axis (*i.e.* the fibre direction) is not aligned with any principal geometric axis, and (ii) a medical scoliosis support brace with non-prismatic geometry and desired compliance axes. Cross-sectional centres would not provide insight into the tape spring behaviour due to the symmetry-breaking tape spring deflection caused by the laminate's extension-shear coupling terms, and are not applicable to the non-prismatic geometry of the scoliosis brace. The stiffness and compliance matrices for both structures are found using a finite element approach, before being decomposed into eigenscrews [7]. Although eigenscrews describe an instantaneous response of the structure, the use of finite element analyses allows this characterisation to be performed at multiple stages throughout a non-linear deformation.

Figure 3 shows the compliance characterisation for the anisotropic cantilevered tape spring, presented in the same manner as in Ref [7]. A follower tip moment has been applied to the POI (located at the centre of the free edge) to cause a large mechanism deflection. Figure 3a shows the initial and deformed shell geometries, the position of the POI during deformation, as well as the positions and orientations of eigenwrenches and eigentwists in the undeformed state. It can be seen that $\hat{T}_2$ and $\hat{T}_3$ are no longer aligned with a geometric axis (unlike the isotropic case in Figure 2), and that the mechanism twists as it deflects. Figures 3b and 3c show the changes in eigenscrew orientations (as seen from the 'North') throughout the deformation. The subplots show half a unit

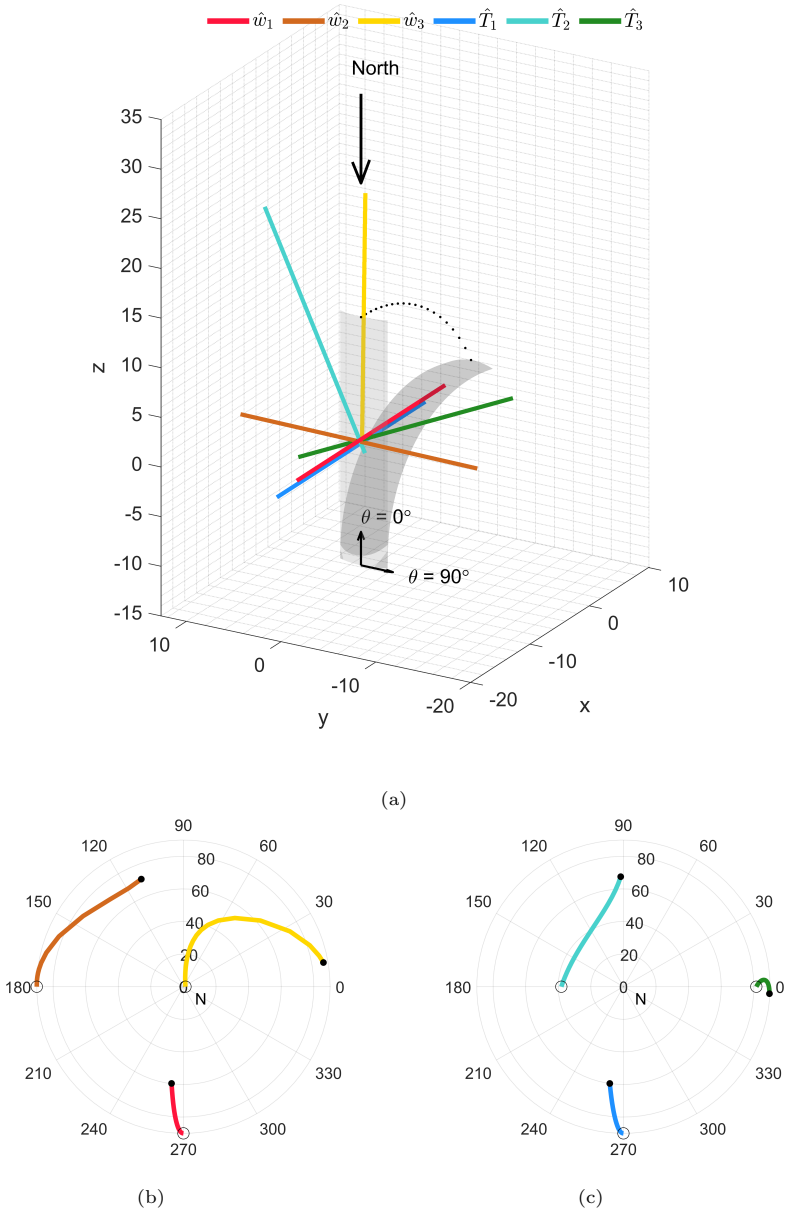

Figure 3: Compliance characterisation of a shallow tape spring with aspect ratio 5, enclosed angle 45° and fibre angle $\theta = 50°$. Shown are (a) the initial and final shell geometries, displacement of the POI, as well as eigenscrews for the undeformed configuration; (b, c) the change of orientation of eigenscrews throughout the shell deformation; initial and final orientations are indicated with ○ and ● respectively.

sphere with the eigenscrew traces (issuing from its centre) plotted on its surface. It can be seen that as the tape spring deflects and twists, some screws change orientation significantly. Information regarding eigenscrew positions and compliance magnitudes has been omitted from Figure 3 for brevity, but can provide additional insight into the compliant mechanism.

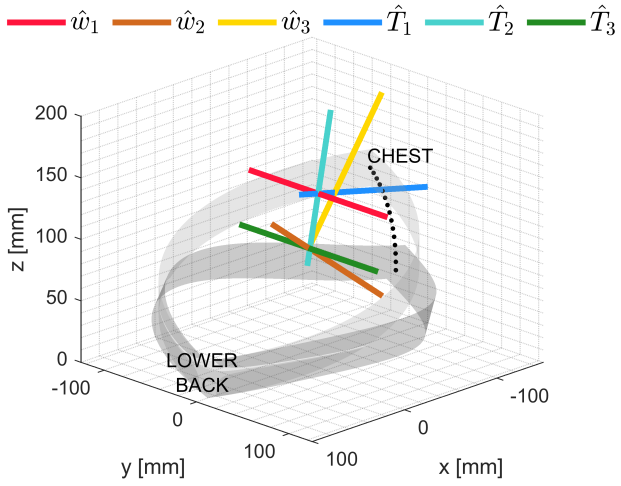

Figure 4: Compliance characterisation of a compliant mechanism for a scoliosis brace based on designs presented in Ref. [32]. Initial and final shell geometries, displacement of the POI, and eigenscrews for the undeformed configuration are shown.

Figure 4 shows the eigenscrew characterisation of a compliant shell mechanism for a scoliosis support brace. The scoliosis brace is comprised of two helical shells, similar to designs shown in Ref. [32], designed to wrap tightly around the patient's torso. The brace provides tailored lateral support to the spine (*i.e.* high stiffness) whilst also offering freedom of movement in other directions (*i.e.* high compliance) such as forward bending around the $\hat{T}_3$ twist axis. To reflect forward bending, a follower tip moment has been applied to a POI located at the top central point where the two helical segments join (chest), while the other ends of the helices are fixed (lower back). Here the principal eigenscrews do not lie on the shell mechanism, but exist at non-trivial positions in the space within the mechanism. Aligning the location and direction of the $\hat{T}_3$ twist axis with the natural bending axis of the wearer is important in increasing patient

comfort. Identifying and visualising the magnitude and location of the eigenscrews is instrumental in the design of a medical scoliosis brace mechanism, as the compliant mechanism must provide support in some directions whilst allowing movement in others. The ability to capture such distinct directional responses using the eigenscrew approach complements the insights that can be gained using traditional structural analysis.

It is worth noting that in the cases presented herein we have focused on the behaviour of a single point on the mechanism, and that the eigenscrew framework may be less insightful for mechanisms whose responses are not clearly defined by a single point, *e.g.* a morphing wing. If insight is required for the global response of the mechanism then multiple decompositions could be computed by considering applied loads at different locations on the mechanism.

6. Conclusions

An analytical link has been shown between the structural mechanics concepts of shear centre and centre of twist and the mechanism design concepts of eigenwrenches and eigentwists. Eigenscrews are shown to align with shear centre and centre of twist positions for a simple isotropic cantilevered tape spring. Eigenscrew characterisations can thus be used to visualise the principal compliance behaviour of a compliant mechanism in cases where cross-sectional centres have less applicability (*e.g.* those with material anisotropy).

Demonstrating the link between these concepts for the special case aids the interpretation of eigenscrew characterisations that are more appropriate for general 3D morphing structures and compliant mechanisms that are well characterised by considering single points of interest. Furthermore, we hope that the demonstrated equivalence will encourage structural engineers to consider the value of the eigenscrew characterisation used in compliant mechanism design, and thus help enable cross-fertilisation of ideas between these fields.

7. Acknowledgements

The work detailed in this brief was funded by the Engineering and Physical Sciences Research Council (EPSRC) as part of the Centre for Doctoral Training in Advanced Composites for Innovation and Science (grant number EP/L016028/1). All data required to reproduce the results shown are provided within this paper.

References

[1] L. Howell, Compliant Mechanisms, John Wiley & Sons Inc., New York, 2001.

[2] H. Lipkin, T. Patterson, Geometrical Properties of Modelled Robot Elasticity: Part I - Decomposition, in: Proceedings of the ASME Design Technical Conferences, Scottsdale AZ, 1992, pp. 179–185.

[3] T. Patterson, H. Lipkin, Structure of Robot Compliance, Journal of Mechanical Design 115 (3) (1993) 576–580.

[4] J. Leemans, C. Kim, W. van de Sande, J. Herder, Unified Stiffness Characterization of Nonlinear Compliant Shell Mechanisms, Journal of Mechanisms and Robotics 11 (1) (2018) 011011. doi:10.1115/1.4041785.

[5] J. Nijssen, G. Radaelli, J. Herder, C. Kim, Overview and Kinetostatic Characterization of Compliant Shell Mechanism Building Blocks, Journal of Mechanisms and Robotics 12 (December) (2020) 061009. doi:10.1115/1.4047344.

[6] C. Kim, On the geometry of stiffness and compliance under concatenation, Journal of Mechanisms and Robotics 12 (2) (2020) 021113. doi:10.1115/1.4045162.

[7] J. Stacey, M. O'Donnell, M. Schenk, C. Kim, Visualising Compliance of Composite Shell Mechanisms, in: Proceedings of the ASME 2020 Inter-

national Design Engineering Technical Conferences and Computers and Information in Engineering Conference, 2020.

[8] C. Bowen, R. Butler, R. Jervis, H. Kim, A. Salo, Morphing and shape control using unsymmetrical composites, Journal of Intelligent Material Systems and Structures 18 (1) (2007) 89–98.

[9] E. Eckstein, A. Pirrera, P. Weaver, Multi-mode morphing using initially curved composite plates, Composite Structures 109 (1) (2014) 240–245. doi:10.1016/j.compstruct.2013.11.005.

[10] E. Lamacchia, A. Pirrera, I. Chenchiah, P. Weaver, Morphing shell structures: A generalised modelling approach, Composite Structures 131 (2015) 1017–1027. doi:10.1016/j.compstruct.2015.06.051.

[11] A. Pirrera, X. Lachenal, S. Daynes, P. Weaver, I. Chenchiah, Multi-stable cylindrical lattices, Journal of the Mechanics and Physics of Solids 61 (11) (2013) 2087–2107. doi:10.1016/j.jmps.2013.07.008.

[12] H. Mallikarachchi, S. Pellegrino, Design of Ultrathin Composite Self-Deployable Booms, Journal of Spacecraft and Rockets 51 (6) (2014) 1811–1821. doi:10.2514/1.A32815.

[13] T. Murphey, W. Davidson, High Strain Composite Folding Truss Structures, in: 2018 AIAA Spacecraft Structures Conference, 2018. doi:10.2514/6.2018-0941.

[14] M. O'Donnell, J. Stacey, I. Chenchiah, A. Pirrera, Multiscale tailoring of helical lattice systems for bespoke thermoelasticity, Journal of the Mechanics and Physics of Solids 133 (2019) 103704. doi:10.1016/j.jmps.2019.103704.

[15] A. Schlothauer, P. Ermanni, Stiff Composite Cylinders for Extremely Expandable Structures, Scientific Reports 9 (1) (2019) 1–8.

[16] C. McHale, D. Hadjiloizi, R. Telford, P. Weaver, Morphing composite cylindrical lattices : Enhanced modelling and experiments, Journal of the Mechanics and Physics of Solids 135 (2020) 1–15. doi:10.1016/j.jmps.2019.103779.

[17] X. Lachenal, S. Daynes, P. Weaver, Review of morphing concepts and materials for wind turbine blade applications, Wind Energy 16 (2) (2013) 283–307. doi:10.1002/we.531.

[18] I. Kuder, A. Arrieta, M. Rist, P. Ermanni, Aeroelastic response of a selectively compliant morphing aerofoil featuring integrated variable stiffness bi-stable laminates, Journal of Intelligent Material Systems and Structures 27 (14) (2016) 1949–1966.

[19] G. Arena, R. Groh, A. Brinkmeyer, R. Theunissen, P. Weaver, A. Pirrera, Adaptive compliant structures for flow regulation, Proceedings of the Royal Society A: Mathematical, Physical and Engineering Sciences 473 (2204) (2017). doi:10.1098/rspa.2017.0334.

[20] O. Stodieck, J. Cooper, P. Weaver, Interpretation of bending/torsion coupling for swept, nonhomogenous wings, Journal of Aircraft 53 (4) (2016) 892–899. doi:10.2514/1.C033186.

[21] T. Megson, Introduction to Aircraft Structural Analysis, 3rd Edition, Butterworth-Heinemann, Amsterdam, 2018.

[22] J. den Hartog, Advanced Strength of Materials, McGraw-Hill, 1952.

[23] S. Timoshenko, J. Goodier, Theory of Elasticity, 3rd Edition, McGraw-Hill, New York, 1970.

[24] U. Andreaus, G. Ruta, A review of the problem of the shear centre(s), Continuum Mechanics and Thermodynamics 10 (6) (1998) 369–380. doi:10.1007/s001610050100.

[25] I. Ecsedi, A. Baksa, Notes on the centre of shear, International Journal of Mechanical Engineering Education 40 (3) (2012) 220–233. doi:10.7227/IJMEE.40.3.6.

[26] M. Chasles, Note Sur Les Propriétés Générales du Système de Deux Corps Semblables Entr'eux et Placés D'un Manière Quelconque Dans L'espace; et Sur le Déplacement Fini, ou Infiniment Petit, D'un Corps Solide Libre, Bulletin Des Sciences Mathématiques, Astronomiques, Physiques et Chimiques 14 (1831) 321–326.

[27] J. Nijssen, G. Radaelli, J. Herder, J. Ring, C. Kim, Spatial Concept Synthesis of Compliant Mechanisms Utilizing Non-Linear Eigentwist Characterization, in: Proceedings of the ASME 2018 International Design Engineering Technical Conferences and Computers and Information in Engineering Conference, 2018. doi:10.1115/detc2018-85307.

[28] B. Goodno, J. Gere, Mechanics of Materials, 9th Edition, Cengage Learning, Boston, 2018.

[29] T. Megson, Structural and Stress Analysis, 4th Edition, Butterworth-Heinemann, Amsterdam, 2019.

[30] A. Nettles, Basic mechanics of laminated composite plates, Tech. Rep. October 1994, NASA Marshall Spaceflight Centre (1994).

[31] N. Ciblak, Analysis of Cartesian Stiffness And Compliance With Applications, Ph.D. thesis, Georgia Institute of Technology (1998).

[32] H. Kooistra, Scoliosis Brace Design: Utilizing Compliant Shell Mechanisms and Primary Compliance Vector Path Optimization, Master thesis, TU Delft (2019).